

An overview of recent STAR jet measurements

Nihar Ranjan Sahoo (for the STAR collaboration)

*Institute of Frontier and Interdisciplinary Science, Shandong University, Qingdao, Shandong,
266237, China*

*Key Laboratory of Particle Physics and Particle Irradiation, Shandong University, Qingdao,
Shandong, 266237, China ,**

These proceedings discuss recent jet measurements by the STAR experiment at RHIC to study jet substructure in $p+p$ and jet quenching in Au+Au collisions at $\sqrt{s_{NN}} = 200$ GeV. Furthermore, STAR's future plans for precision jet measurements with the upcoming data-taking periods in 2023-2025 are presented.

Keywords: Quark-Gluon Plasma; heavy-ion collisions; QCD; jet.

1. Introduction

Jets in $p+p$ and heavy-ion collisions arise from hard-scattered (high- Q^2) quarks and gluons of the incoming beams. In vacuum, a highly virtual parton generated in such interaction comes on-shell by radiating gluons, resulting in a jet shower. Studying jet properties in $p+p$ collisions provides the opportunity to explore the perturbative and non-perturbative QCD effects in vacuum. In addition, the comparison between data and different QCD-based Monte Carlo (MC) event generators helps to constrain model parameters. In heavy-ion collisions, a highly energetic parton—while traversing through the Quark-Gluon Plasma (QGP)—interacts with the colored medium and loses its energy via medium-induced gluon radiation. This phenomenon is known as the jet quenching.¹ Suppression of jet yield, modification of jet shape and substructure, and jet deflection in the QGP are the manifestations of jet quenching in heavy-ion collisions.

In these proceedings we present recent jet measurements by the STAR experiment at RHIC, addressing jet substructure in $p+p$ collisions and jet quenching in Au+Au collisions.

2. Jet measurements in $p+p$ collisions

The fragmentation and evolution of a hard-scattered parton is described by the Dokshitzer-Gribov-Lipatov-Altarelli-Parisi (DGLAP) splitting kernels.⁷⁻⁹ This

*nihar@sdu.edu.cn, nihar@rcf.rhic.bnl.gov

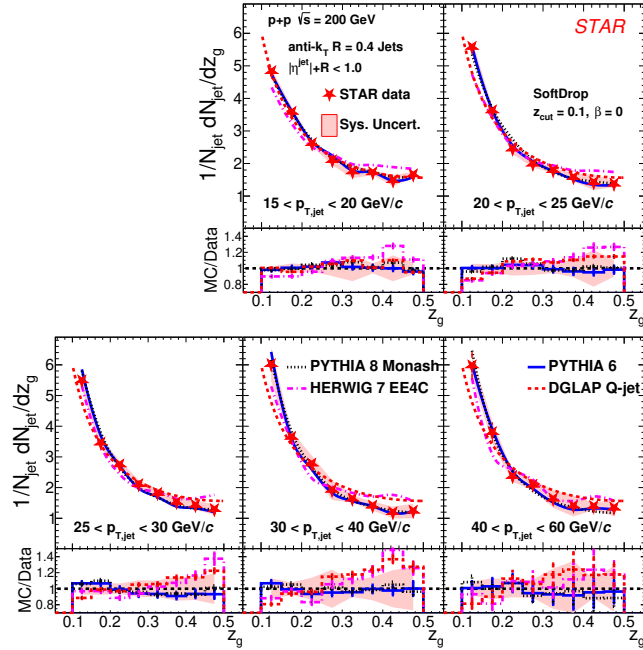


Fig. 1. The z_g distributions for different $p_{T,jet}$ in $p+p$ collisions at $\sqrt{s} = 200$ GeV.⁴

splitting probability depends on the momentum fraction of the split and the opening angle, and can be studied in $p+p$ collisions. In QCD, higher order corrections contribute to the jet mass and substructure observables. To study these observables in STAR, jets are studied by clustering charged tracks from the time projection chamber and neutral particles from the barrel electromagnetic calorimeter towers using the anti- k_T jet reconstruction algorithm² with different resolution parameters (R) between 0.2 and 0.6. Furthermore, such measurements in $p+p$ collisions provide a baseline for the similar measurements in heavy-ion collisions to study the modification of parton shower in the finite-temperature QCD medium.

2.1. *SoftDrop jet grooming*

The SoftDrop jet-grooming^{3,10,11} algorithm helps to study jet substructure by suppressing soft large-angle radiations. In this procedure, the soft and wide-angle radiations are removed sequentially from the jet de-clustering tree. This is achieved using the Cambridge/Aachen (C/A) clustering algorithm² by de-clustering jet branching history with removing the soft branch until it satisfies the condition:

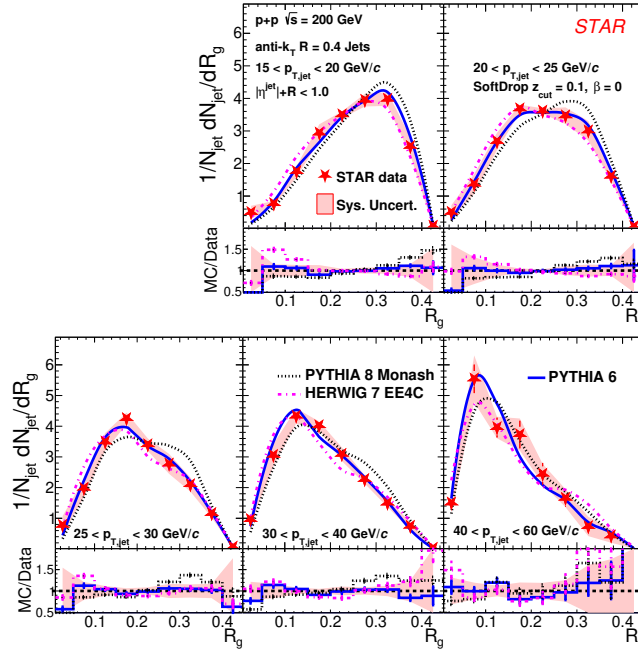


Fig. 2. The R_g distributions for different $p_{T,jet}$ in $p+p$ collisions at $\sqrt{s} = 200$ GeV.⁴

$$z_g = \frac{\min(p_{T,1}, p_{T,2})}{p_{T,1} + p_{T,2}} > z_{cut} \left(\frac{R_g}{R} \right)^\beta. \quad (1)$$

In Eq. (1), indices 1 and 2 represent the two sub-jets of splitting. The radius (R) is the distance in pseudorapidity and azimuthal angle space between two sub-jets, and R_g is the groomed jet radius. The SoftDrop threshold $z_{cut} = 0.1$, and angular exponent $\beta = 0$ are used for this de-clustering procedure for infrared and collinear (IRC) safety.¹¹

At RHIC, the first fully corrected SoftDrop observables, z_g and R_g , are measured in $p+p$ collisions at $\sqrt{s} = 200$ GeV by the STAR experiment for inclusive jets with $R = 0.2, 0.4$, and 0.6 , and $15 < p_{T,jet} < 60$ GeV/ c .⁴ Figures 1 and 2 show the distributions of z_g and R_g , respectively. The shape of z_g distributions indicates no $p_{T,jet}$ dependence above 30 GeV/ c , and they are more asymmetric than the DGLAP splitting function for a leading order quark emitting a gluon. R_g distributions reveal a narrowing with increasing $p_{T,jet}$, and the splitting is asymmetric at high $p_{T,jet}$. The STAR-tuned⁶ PYTHIA-6 with Perugia 2012 well describes the jet substructure observables at this energy. The comparisons with MC event generator

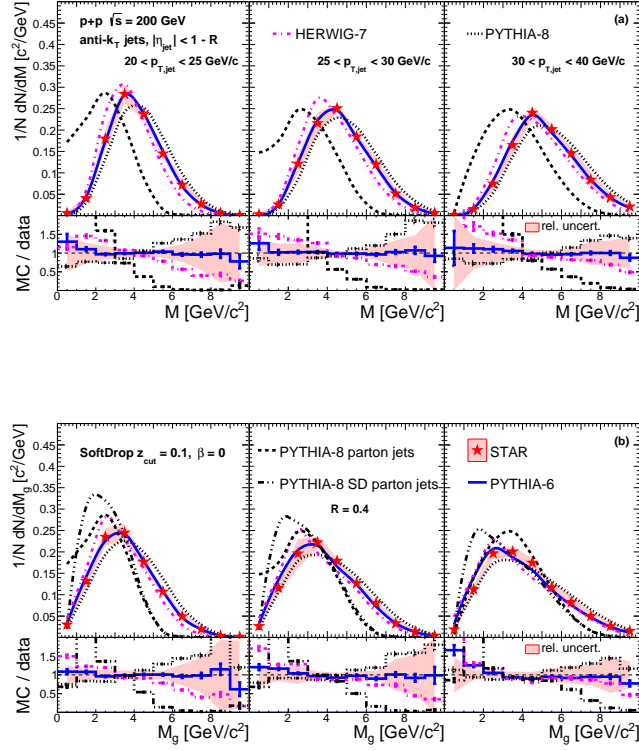


Fig. 3. Jet mass distributions for different $p_{T,\text{jet}}$ and jet R in $p+p$ collisions at $\sqrt{s} = 200$ GeV.⁵

predictions help further study different hadronization models for the higher-order QCD corrections at RHIC energy.

2.2. Jet mass

The mass of quark or gluon jets is sensitive to the fragmentation of highly virtual parent partons. The SoftDrop grooming procedure removes soft and wide-angle radiations from jets making the groomed jets less sensitive to the higher order QCD corrections. Jet mass is defined as the four-momentum sum of jet constituents, $M = |\sum_{i \in \text{jet}} p_i| = \sqrt{E^2 - \mathbf{p}^2}$. Here E and \mathbf{p} are the energy and three-momentum of the jet, respectively. Studying both ungroomed and groomed jets, and comparing to different MC event generators can provide information on different pQCD effects and fragmentation. The STAR experiment has reported the first fully corrected ungroomed (M) and groomed (M_g) mass distributions of inclusive jets for several values of R at $\sqrt{s} = 200$ GeV as shown in Fig 3.⁵ These jets are selected

within the range of $30 < p_{T,\text{jet}} < 40$ GeV/ c . It is observed that the mean and width of the jet mass increases with increasing R due to the inclusion of wide-angle radiation. The same trend is also seen with growing $p_{T,\text{jet}}$ that increases the radiation phase space. The groomed jet mass distribution gets shifted to a smaller value than that of ungroomed mass due to the reduction of soft radiation in the SoftDrop grooming procedure. The LHC-tuned PYTHIA-8 and HERWIG-7 EE4C MC event generators over- and under-predicts the jet mass at RHIC, respectively, whereas the STAR-tuned PYTHIA-6 quantitatively describes the data. This observation is similar to that for the R_g observable as discussed in the previous subsection. These measurements serve as a reference for future jet mass measurements in heavy-ion collisions at RHIC.

3. Jet quenching measurements in Au+Au collisions

The STAR experiment has reported measurements of jet quenching using observable high- p_T hadron suppression¹² and dihadron correlations.^{13,14} The hadronic measurements have limited information on the underlying mechanism of jet quenching due to the final-state effects in heavy-ion collisions. Over the last few years, the application of jet reconstruction algorithms and the development of methods for rigorous correction of uncorrelated background in heavy-ion collisions enable us to study jet quenching in more detail using fully reconstructed jets.

The first measurements of inclusive jet, semi-inclusive hadron+jet, and preliminary results of γ_{dir} +jet and π^0 +jet measurements have been reported by the STAR experiment. The measurement techniques and their results are discussed in this section.

3.1. Inclusive jet suppression

Jet measurements in heavy-ion collisions are complicated due to the presence of large uncorrelated background. For the inclusive jet spectrum measurements in STAR, jets are reconstructed using anti- k_T algorithm² with an additional requirement of a high- p_T hadronic constituent ($p_{T,\text{lead}}^{\text{min}}$), in order to identify jets from hard scattering processes. The selection of $p_{T,\text{lead}}^{\text{min}}$ should satisfy the following criteria: i) it must be sufficiently high so that contributions from combinatorial jets are negligible; ii) the probability of multiple constituents with $p_T \geq p_{T,\text{lead}}^{\text{min}}$ is negligible; iii) this $p_{T,\text{lead}}^{\text{min}}$ cut does not introduce a selection bias on the jet population within the considered $p_{T,\text{jet}}$ range. Using this technique, the first fully corrected inclusive jet spectra in central and peripheral Au+Au collisions at $\sqrt{s_{\text{NN}}} = 200$ GeV have been reported with $p_{T,\text{lead}}^{\text{min}} = 5$ GeV/ c .¹⁵

The nuclear modification factor (R_{AA}) is defined as the ratio of inclusive charged jet yield in central Au+Au collisions to its cross sections in $p+p$ collisions scaled by the nuclear thickness factor $\langle T_{\text{AA}} \rangle$ of central collisions. Similarly, R_{CP} is defined

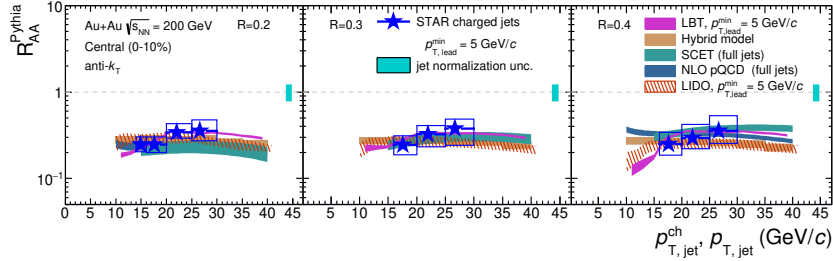


Fig. 4. R_{AA}^{Pythia} as a function of $p_{T,\text{jet}}^{\text{ch}}$ in 0-10% central Au+Au collisions and for different jet R at $\sqrt{s_{NN}} = 200$ GeV.¹⁵

considering 60-80% peripheral collisions as a reference instead of $p+p$ collisions. For R_{AA} , PYTHIA is used as a vacuum reference, hence it is labeled as R_{AA}^{Pythia} . Figure 4 shows the R_{AA}^{Pythia} as a function of $p_{T,\text{jet}}^{\text{ch}}$ for inclusive jets with $R = 0.2, 0.3$ and 0.4 within $15 < p_{T,\text{jet}}^{\text{ch}} < 30$ GeV/ c . Strong suppression is observed in 0-10% central Au + Au collisions, and no jet R dependence of the suppression is seen. Different theory calculations^{16–20} are consistent with the data. The R_{CP} shows strong and similar suppressions for $R = 0.2$ and 0.3 jets as shown in Fig 5. The yields of inclusive charged hadrons and jets show a comparable level of suppression within the same p_T interval in central Au+Au collisions at $\sqrt{s_{NN}} = 200$ GeV. In addition, the comparison between central Au+Au collisions at RHIC and central Pb+Pb collisions at the LHC—although within different p_T intervals—show a similar magnitude of suppression for charged hadrons and jets yields. The medium-induced broadening of the inclusive jet is measured by taking the ratio of inclusive jet yields for $R = 0.2$ and 0.4 . No significant modification of the transverse jet profile due to jet quenching is observed for the inclusive jet population in central Au+Au collisions at $\sqrt{s_{NN}} = 200$ GeV and is consistent with the LHC data. The ongoing full jet analysis will access the inclusive jet suppression measurement at higher $p_{T,\text{jet}}$ at RHIC energies.

3.2. Semi-inclusive $\gamma_{\text{dir}}+\text{jet}$ and hadron+jet suppression

The STAR experiment published²¹ the measurement of semi-inclusive distribution of reconstructed recoil jets from a high- p_T trigger hadron (h+jet) in Au+Au collisions. In this measurement, the uncorrelated background contribution is mitigated by using a novel mixed-event (ME) technique. It is found that the contributions from multi-parton interactions in the recoil acceptance are negligible.

The semi-inclusive h+jet measurement enables us to perform similar $\gamma_{\text{dir}}+\text{jet}$ and $\pi^0+\text{jet}$ measurements in STAR by combining the method used in the previous $\gamma_{\text{dir}}+\text{hadron}$ and $\pi^0+\text{hadron}$ correlation measurements.²² In this measurement, γ_{dir} and π^0 are within the trigger energy ranges of $9 < E_T^{\text{trig}} < 20$ GeV and $9 < E_T^{\text{trig}} <$

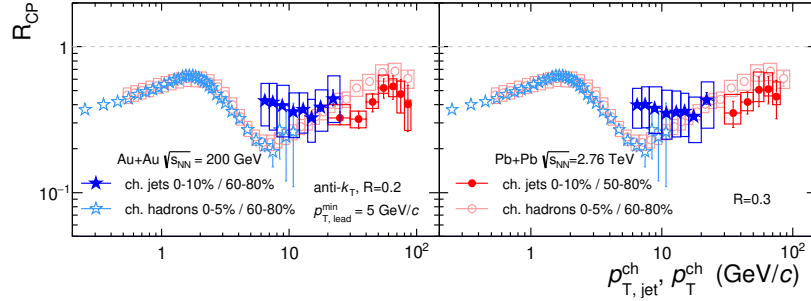


Fig. 5. R_{CP} as a function of $p_{T,jet}$ in Au+Au collisions and for different jet R at $\sqrt{s_{NN}} = 200$ GeV.¹⁵

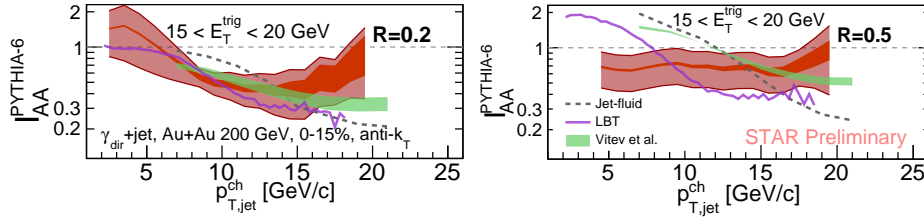


Fig. 6. $\gamma_{dir}+jet$ I_{AA} as a function of $p_{T,jet}$ for $R = 0.2$ and 0.5 at $\sqrt{s_{NN}} = 200$ GeV.²⁴

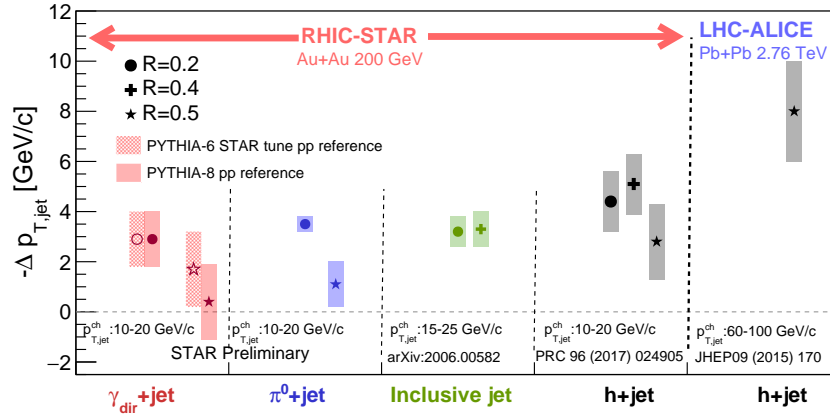


Fig. 7. $-\Delta p_{T,jet}$ for different observables measured at RHIC and the LHC.²⁴

15 GeV, respectively. However, in these proceedings only $\gamma_{dir}+jet$ results with $15 < E_T^{trig} < 20$ GeV range is discussed, which is the highest E_T^{trig} range measured in

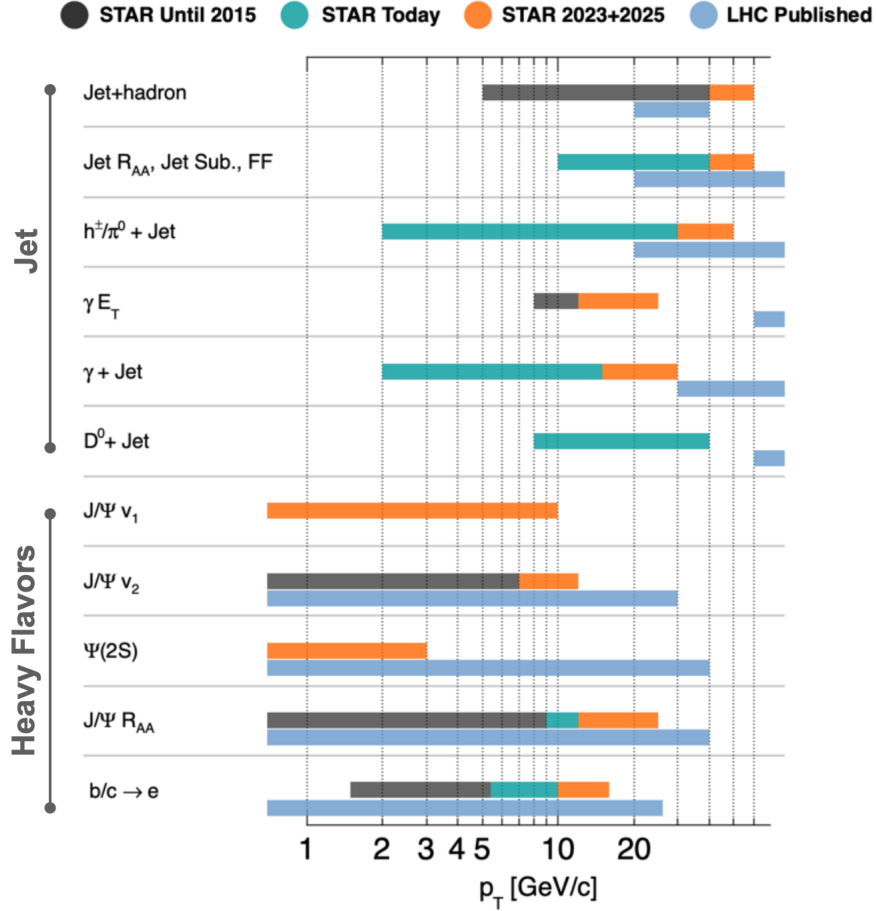


Fig. 8. The kinematic coverages of the STAR hard probe measurements (past, current, and future projection) are shown and compared to the LHC (published) measurements.²⁵

this analysis. Recoil jets are measured using anti- k_T algorithm with $R = 0.2$ and 0.5 . The same ME technique as in h+jet paper is applied to subtract uncorrelated jet background. The unfolding procedure, as in h+jet paper, is applied to correct for the detector effects and heavy-ion background fluctuations. Finally, the ratio of recoil jet yield in central Au+Au collisions to that of PYTHIA-8, I_{AA}^{PYTHIA} , is presented for the aforementioned jet radii. The I_{AA}^{PYTHIA} of $\gamma_{\text{dir}}+\text{jet}$ for $R = 0.2$, within $15 < E_T^{\text{trig}} < 20$ GeV, shows a stronger suppression than that of $R = 0.5$ as shown in Fig. 6, which hints at a potential R dependence of recoil jet suppression at RHIC. The upcoming results with the $p+p$ data as a reference will be reported

in the final publication of this measurement. Precision measurement with extended recoil jet $p_T^{\text{jet, ch}}$ range for $\gamma_{\text{dir}}+\text{jet}$ is planned with the upcoming RHIC runs.

3.3. Charged jet $p_{T,\text{jet}}$ spectrum shift: RHIC vs. LHC

Jet suppression is commonly reported via R_{AA} and I_{AA} as a function of $p_{T,\text{jet}}$. These observables convolute the effect of energy loss with the shape of the jet $p_{T,\text{jet}}$ spectrum. In order to deconvolute this, a $p_{T,\text{jet}}$ shift ($-\Delta p_{T,\text{jet}}$ in Fig. 7) is measured for a quantitative comparison of jet energy loss from different observables. The STAR h+jet,²¹ inclusive jet, preliminary $\gamma_{\text{dir}}+\text{jet}$, and $\pi^0+\text{jet}$ measurements, and ALICE h+jet²³ measurements report values of $-\Delta p_{T,\text{jet}}$, although within different kinematic ranges. While comparing these values as shown in Fig. 7, an indication of smaller in-medium energy loss at RHIC than the LHC is seen.

4. STAR ongoing measurements and upcoming data-taking plan

There are several ongoing jet measurements in STAR to study the QGP medium properties in heavy-ion collisions, such as full jet reconstruction to extend the $p_{T,\text{jet}}$ reach, jet fragmentation function, jet shape, heavy-flavor jet, and recoil jet azimuthal angular correlation with trigger particles.

The STAR experiment plans to take high statistics data of Au+Au collisions at $\sqrt{s_{NN}} = 200$ GeV in 2023 and 2025, and $p+p$ collision data at $\sqrt{s} = 200$ GeV along with $p+A$ collisions in 2024 with 28 cryo-weeks for each year.²⁵ The kinematic coverages of various measurements related to hard probes using these datasets are presented in Fig 8. These datasets are crucial for studying the inner-workings of QGP utilizing precision jet measurements.

5. Summary

The STAR experiment has recently reported important results on jet substructure observables in $p+p$ collisions, and various jet quenching observables in heavy-ion collisions to study QGP properties. Several other jet measurements are ongoing and will be presented in the near future. Besides, STAR's upcoming data-taking (during 2023-2025 RHIC runs) is crucial for the precision jet measurements with large kinematic coverages, whereas high statistics $p+p$ data (2024 RHIC run) are important for providing high precision references.

Acknowledgement

NRS is supported by the Fundamental Research Funds of Shandong University and NNSF of China:12050410235.

References

1. L. Cunqueiro and A. M. Sickles, [arXiv:2110.14490 [nucl-ex]].

10 *Nihar Sahoo*

2. G. P. Salam, Eur. Phys. J. C **67**, 637-686 (2010) doi:10.1140/epjc/s10052-010-1314-6 [arXiv:0906.1833 [hep-ph]].
3. A. J. Larkoski, S. Marzani and J. Thaler, Phys. Rev. D **91**, no.11, 111501 (2015) doi:10.1103/PhysRevD.91.111501 [arXiv:1502.01719 [hep-ph]].
4. J. Adam *et al.* [STAR], Phys. Lett. B **811**, 135846 (2020) doi:10.1016/j.physletb.2020.135846 [arXiv:2003.02114 [hep-ex]].
5. M. Abdallah *et al.* [STAR], Phys. Rev. D **104**, no.5, 052007 (2021) doi:10.1103/PhysRevD.104.052007 [arXiv:2103.13286 [hep-ex]].
6. J. Adam *et al.* [STAR], Phys. Rev. D **100**, no.5, 052005 (2019) doi:10.1103/PhysRevD.100.052005 [arXiv:1906.02740 [hep-ex]].
7. V. N. Gribov and L. N. Lipatov, Sov. J. Nucl. Phys. **15**, 438-450 (1972) IPTI-381-71.
8. Y. L. Dokshitzer, Sov. Phys. JETP **46**, 641-653 (1977)
9. G. Altarelli and G. Parisi, Nucl. Phys. B **126**, 298-318 (1977) doi:10.1016/0550-3213(77)90384-4
10. M. Dasgupta, A. Fregoso, S. Marzani and G. P. Salam, JHEP **09**, 029 (2013) doi:10.1007/JHEP09(2013)029 [arXiv:1307.0007 [hep-ph]].
11. A. J. Larkoski, S. Marzani, G. Soyez and J. Thaler, JHEP **05**, 146 (2014) doi:10.1007/JHEP05(2014)146 [arXiv:1402.2657 [hep-ph]].
12. C. Adler *et al.* [STAR], Phys. Rev. Lett. **89**, 202301 (2002) doi:10.1103/PhysRevLett.89.202301 [arXiv:nucl-ex/0206011 [nucl-ex]].
13. C. Adler *et al.* [STAR], Phys. Rev. Lett. **90**, 082302 (2003) doi:10.1103/PhysRevLett.90.082302 [arXiv:nucl-ex/0210033 [nucl-ex]].
14. J. Adams *et al.* [STAR], Phys. Rev. Lett. **97**, 162301 (2006) doi:10.1103/PhysRevLett.97.162301 [arXiv:nucl-ex/0604018 [nucl-ex]].
15. J. Adam *et al.* [STAR], Phys. Rev. C **102**, no.5, 054913 (2020) doi:10.1103/PhysRevC.102.054913 [arXiv:2006.00582 [nucl-ex]].
16. I. Vitev and B. W. Zhang, Phys. Rev. Lett. **104**, 132001 (2010) doi:10.1103/PhysRevLett.104.132001 [arXiv:0910.1090 [hep-ph]].
17. Y. T. Chien and I. Vitev, JHEP **05**, 023 (2016) doi:10.1007/JHEP05(2016)023 [arXiv:1509.07257 [hep-ph]].
18. J. Casalderrey-Solana, D. Gulhan, G. Milhano, D. Pablos and K. Rajagopal, JHEP **03**, 135 (2017) doi:10.1007/JHEP03(2017)135 [arXiv:1609.05842 [hep-ph]].
19. Y. He, T. Luo, X. N. Wang and Y. Zhu, Phys. Rev. C **91**, 054908 (2015) [erratum: Phys. Rev. C **97**, no.1, 019902 (2018)] doi:10.1103/PhysRevC.91.054908 [arXiv:1503.03313 [nucl-th]].
20. W. Ke, Y. Xu and S. A. Bass, Phys. Rev. C **100**, no.6, 064911 (2019) doi:10.1103/PhysRevC.100.064911 [arXiv:1810.08177 [nucl-th]].
21. L. Adamczyk *et al.* [STAR], Phys. Rev. C **96**, no.2, 024905 (2017) doi:10.1103/PhysRevC.96.024905 [arXiv:1702.01108 [nucl-ex]].
22. L. Adamczyk *et al.* [STAR], Phys. Lett. B **760**, 689-696 (2016) doi:10.1016/j.physletb.2016.07.046 [arXiv:1604.01117 [nucl-ex]].
23. J. Adam *et al.* [ALICE], JHEP **09**, 170 (2015) doi:10.1007/JHEP09(2015)170

- [arXiv:1506.03984 [nucl-ex]].
24. N. R. Sahoo [STAR], PoS **HardProbes2020**, 132 (2021) doi:10.22323/1.387.0132 [arXiv:2008.08789 [nucl-ex]].
 25. STAR BUR: <https://indico.bnl.gov/event/11308/>